Comparative study of soft thermal printing and lamination of dry thick photoresist films for the uniform fabrication of polymer MOEMS on small-sized samples

Sami Abada, Laurène Salvi, Rémi Courson, Emmanuelle Daran, Benjamin Reig, Jean-Baptiste Doucet, Thierry Camps, Véronique Bardinal

Comparison of lamination and soft thermal printing of dry thick photoresist films for the uniform fabrication of polymer MOEMS on small-sized samples

S. Abada, L. Salvi, R. Courson, E. Daran, B. Reig, JB Doucet, T. Camps and V. Bardinal

CNRS, LAAS, Univ de Toulouse, 7 avenue du colonel Roche, F-31400 Toulouse, France

E-mail: bardinal@laas.fr

Abstract. A method called "soft thermal printing" (STP) was developed to ensure the optimal transfer of 50-µm-thick dry epoxy resist films (DF-1050) on small-sized samples. The aim was the uniform fabrication of high aspect ratio polymer-based MOEMS (micro-optical-electrical-mechanical system) on small and/or fragile samples, such as GaAs. The printing conditions were optimized, and the resulting thickness uniformity profiles were compared to those obtained via lamination and SU-8 standard spin-coating. Under the best conditions tested, STP and lamination produced similar results, with a maximum deviation to the central thickness of 3% along the sample surface, compared to greater than 40% for SU-8 spin-coating. Both methods were successfully applied to the collective fabrication of DF1050-based MOEMS designed for the dynamic focusing of VCSELs (vertical-cavity surface-emitting lasers). Similar, efficient electro-thermo-mechanical behaviour was obtained in both cases.

Keywords: dry thick resist film, SU-8, thickness uniformity, lamination, wafer-scale fabrication, MOEMS, micro-optics

1. Introduction

1.1. Motivations: VCSEL beam shaping

VCSELs (vertical-cavity surface-emitting lasers) are near infrared semiconductor laser diodes that exhibit many advantages, such as parallel operation, low threshold, circular beam and high modulation rate. As a result, they have become the first choice as sources for short distance optical links and for optical mice sensors [1]. In recent years, SU-8 negative-tone photoresist has been used not only for microfluidic moulds and MEMS (micro-electro-mechanical systems) fabrication [4][5][6] but also for microlens integration on VCSEL sources [8][9][10]. This is due to the unique thermal, mechanical and optical properties of this epoxy resist that enables the definition of transparent, thick (up to 1 mm) and high aspect ratio microstructures via UV photolithography. Direct integration of polymer microlenses on the VCSEL surface is a promising way to reduce beam divergence and to further improve device integration in optical systems. In particular, dynamic focusing of the VCSEL beam is of great interest for the fabrication of compact optical sensors that require a real-time scan of the laser beam position. To this end, a polymer-based MOEMS that can be collectively integrated on a VCSEL at a post-process stage and with an alignment precision given by photolithography (1 μm) was reported by the authors. The MOEMS is composed of a suspended SU-8 membrane associated with a polymer microlens (figure 1). It provides efficient vertical displacement of the microlens plane under electro-thermal actuation (~8 μm for 42 mW) [2]. The initial distance between the microlens and the VCSEL is controlled by the height of the polymer MEMS. Taking into account the numerical aperture of the VCSEL and the microlens that can be deposited on the top surface, the height has to be equal to 100±8 μm to make efficient beam focusing possible [3]. The MOEMS height has to be identical for all devices to ensure uniform operation of the final arrays on the wafer. Furthermore, as this MOEMS is fabricated via a double UV exposure method in a single thick

negative photoresist layer, SU-8 (see section 4.1), sufficient flatness of the resist is necessary to achieve good control of the successive alignments. However, standard spin-coating of highly viscous resists, such as SU-8, is known to create annular edge beads at the sample periphery that can be higher than 30 µm for a targeted height of 100 µm. This induces the creation of an air gap between the photomask and the resist, leading to optical diffraction effects during the UV photolithography step and to poor pattern definition. Moreover, edge beads are responsible for the large thickness inhomogeneity of the final patterns, which is not acceptable for a precise wafer-scale fabrication. This problem is more critical in the case of small-sized samples, for which edge beads cover a large part of the total surface, such as GaAs optoelectronic device wafers (with a maximum size that does not exceed 3 inches in diameter).

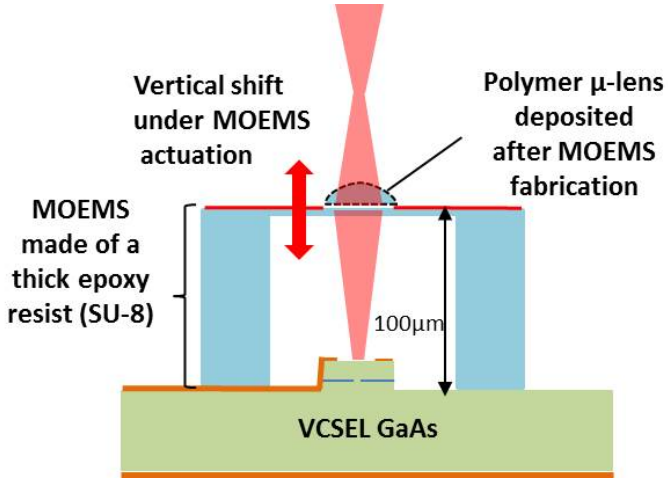

Figure 1: Principle of polymer-based MOEMS integration on a VCSEL for beam shaping.

1.2. Methods for improving the thickness uniformity during spin-coating

Several methods have been reported in the literature to overcome the detrimental effects of the thickness inhomogeneity caused by spin-coating. One consists of filling the air gap with glycerol to ensure index matching during UV photolithography [11]. The use of a soft cushion to flatten the resist during UV exposure was also reported [12]. Projection lithography has also been used [13]. Although these solutions significantly reduce the diffraction effects, they do not provide sufficient control of the SU-8 final thickness. For example, for direct fabrication of SU-8-based static or movable lenses on VCSEL wafers,

the tolerance error on the distance between the VCSEL and the lens is less than 8 µm (for a target value of 100 µm) [10][1]. Other well-known solutions are based on manual or automatic elimination of edge beads during spinning, but this process significantly reduces the usable surface. Therefore, it is not applicable to small and/or non-circular samples. Nevertheless, this method can be combined with an artificial increase of the sample surface by temporarily gluing it near surrounding pieces of sample (with the same thickness) on an adhesive support just before the spin- coating step [14]. In this way, the edge beads can extend the boundaries, provided close contact is obtained between the sample and the surrounding pieces; however, this is only applicable to rectangular samples. Finally, advanced treatments proposed by Microchem™, such as edge bead remover (EBR), significantly improve layer uniformity from 50% to 11.3% [15], although it can sometimes lead to de-wetting effects.

1.3. Alternatives to spin-coating: lamination and soft thermal printing

Avoiding spin-coating is a promising way to solve the inhomogeneity problem. This can be achieved using several techniques, such as gravity dispense [16][16], spray-coating [18] and dry resist film lamination [19][20]. Gravity dispense requires exact knowledge of the sample dimensions and is only applicable to flat surfaces. Spray-coating is not suitable for resist thicknesses greater than 25 µm. Finally, lamination involves placing the sample surface in contact with a uniform dry thick resist film (previously fabricated on a large flexible sheet called a "liner") between two rotating rollers that can be heated and independently controlled (Figure 2). This technique is not easy to apply in some cases, for example, with brittle samples, such as GaAs, that can be weakened after passing between the two rotating rollers under high pressure. If the applied pressure is lowered to avoid this problem, adhesion on the surface becomes poor, so a pressure trade-off has to be found.

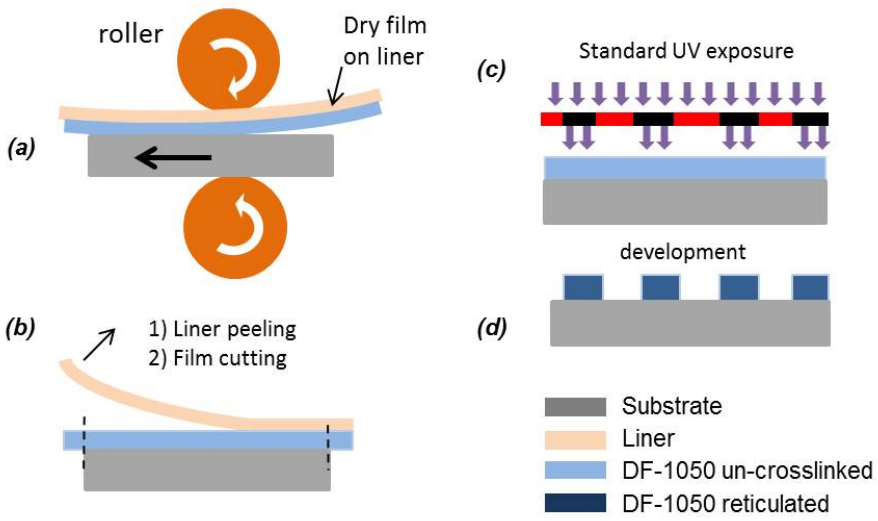

Figure 2: Process of dry film lamination: (a) Lamination between the two rotating rollers (2.5 bars and 0.5 m/min), (b) Film cutting and liner peeling, (c) Irradiation and baking, and (d) Development.

The authors recently developed a "softer" method, called "soft thermal printing" (STP), based on the use of a nanoimprint setup [21]. As a result of the homogeneous pressure and uniform heating that can be applied via this method, the feasibility of the transfer of a "homemade" 100-µm-thick dry SU-8 film (previously spun on a large surface liner) was demonstrated on a quarter of a silicon wafer of 4 inches in diameter. The thickness variation along the sample was decreased from 40% to 15%. However, further optimization was not possible because of the poor film reproducibility.

In this work, for the first time, we combine STP with the use of a commercial photoresist dry film, namely, DF-1050 (Engineered Material Systems) **Erreur ! Source du renvoi introuvable.**. Interest in this dry film was previously demonstrated for microfluidics applications using lamination [21]. It presents similar mechanical and optical properties as SU-8, and it is much easier to implement since it has a calibrated thickness regardless of the film size. Furthermore, its implementation is less time-consuming and significantly cheaper. A full comparative study of the uniformity profiles given by lamination and by STP of DF-1050 films on small-sized samples (less than 1 inch in diameter) is presented. Furthermore,

STP and lamination are applied to the fabrication of DF-1050-based MOEMS on GaAs samples via double film transfer combined with a new planar double UV exposure process.

2. Principle of Soft Thermal Printing and operating procedure

STP is based on the use of nanoimprint lithography (NIL) instrumentation (Nanonex NX-2500) originally dedicated to thermal or UV NIL[22]. This setup is equipped with a double flexible membrane system enabling "soft" film transfer through homogeneous isostatic pressure applied to the substrate. The sample to be processed can be flat or already micro-structured, and its maximum size is 6 inches in diameter. A standard surface treatment, such as oxygen plasma, is performed before printing to render the wafer surface hydrophilic, as is generally done before SU-8 spin-coating. The operating procedure is shown in figure 3. First, a piece of dry thick DF1050-film is cut at room temperature to fit the sample size (a). In the case of STP, the film can be precisely positioned on the surface before placing the assembly between the flexible membranes of the nanoimprint setup (see image in Fig. 3). In this way, there is no cutting step applied to the sample after transfer, which is an additional advantage over lamination for processing fragile samples. Second, the film and the sample are put into contact under vacuum. Soft thermal printing is then achieved under uniform pressure and temperature, leading to conformal transfer (b). After printing, the liner is peeled off (c). To define the microscale patterns, standard UV exposure is performed at 365 nm using a MA6 mask aligner (i-line with a broadband filter, 256 mJ/cm²), followed by a standard post-exposure bake at 100°C for 6 min (d). After development in cyclohexanone (6 min), the thickness of the final posts can be measured using mechanical profilometry along the sample axis (e) with a precision of 0.2 µm. In the first part of this work, STP is applied to the transfer of DF-1050 dry resist films with a calibrated nominal thickness (50±3 µm) on a series of identical small-sized silicon square samples (surface 25x25 mm²) to compare with lamination. A specific photomask composed of a 300-µm-period high-density array of square patterns (side length: 100 µm) was used. For each sample

corresponding to each tested condition, the pattern height profile could be systematically extracted and averaged from measurements performed along two orthogonal axes of the sample (f).

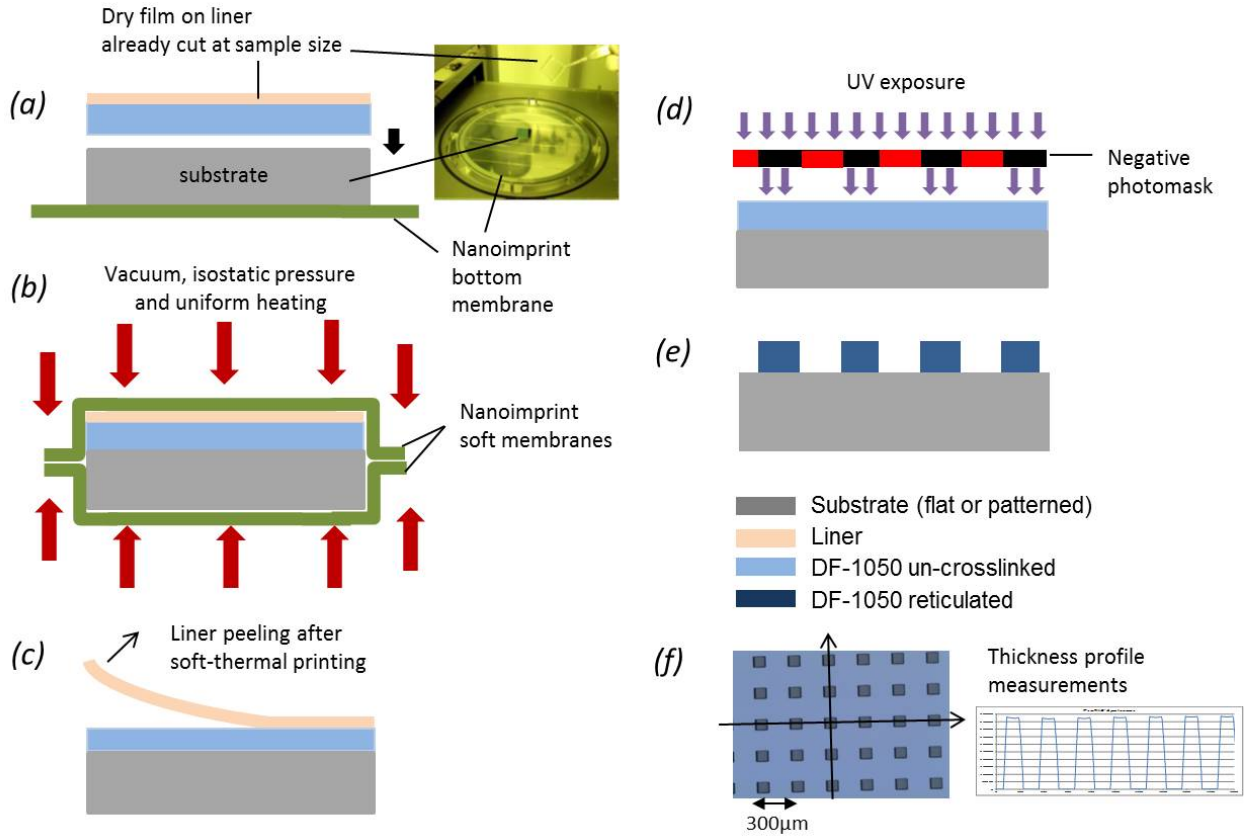

Figure 3: Principle of soft thermal printing of a dry film using nanoimprint equipment with a double membrane system: (a) Film cutting and positioning on the sample, (b) soft thermal printing between the two flexible membranes, (c) liner peel off, (d) UV photolithography, and (e) development. Samples are characterized by optical microscopy, and the uniformity profiles are extracted from mechanical profilometry measurements of the patterns' height (f).

3. Comparative study

3.1. Optimization of the soft thermal printing (STP) conditions

Preliminary work led by the authors on the STP of "homemade" SU-8 dry films was performed with an applied pressure of 80 psi (5.5 bars), a printing time of 30 s and a printing temperature of 60°C [20]. In the present study, the printing conditions had to be adapted to dry DF-1050 films, which have a much lower solvent content than homemade SU-8 dry films. The applied pressure was thus lowered to 15 psi

(1.1 bars) with no detrimental effect on film adhesion with a slightly longer printing time (1 min). Three printing temperatures were tested: 40°C, 50°C and 60°C. After fabrication of identical samples (25x25 mm²) for each condition, the pattern height was measured at the sample centre and was found to be systematically lower than the nominal value regardless of the temperature (Fig. 4). However, this small difference was not significant and could be accounted for by the tolerance on the initial thickness given by the film manufacturer (±3 µm). The thickness variation profile measured along the sample was more relevant. It was found to significantly evolve with printing temperature, with minimal edge beads observed for the lowest temperature, i.e., 40°C. In this case, the maximum deviation to the thickness measured at the centre was 1.4 µm. Finally, SEM images of the final posts showed good pattern definition, vertical sidewalls, and no delamination, regardless of the applied temperature. Consequently, the optimal temperature for STP of DF-1050 films was fixed to 40°C for the rest of the study.

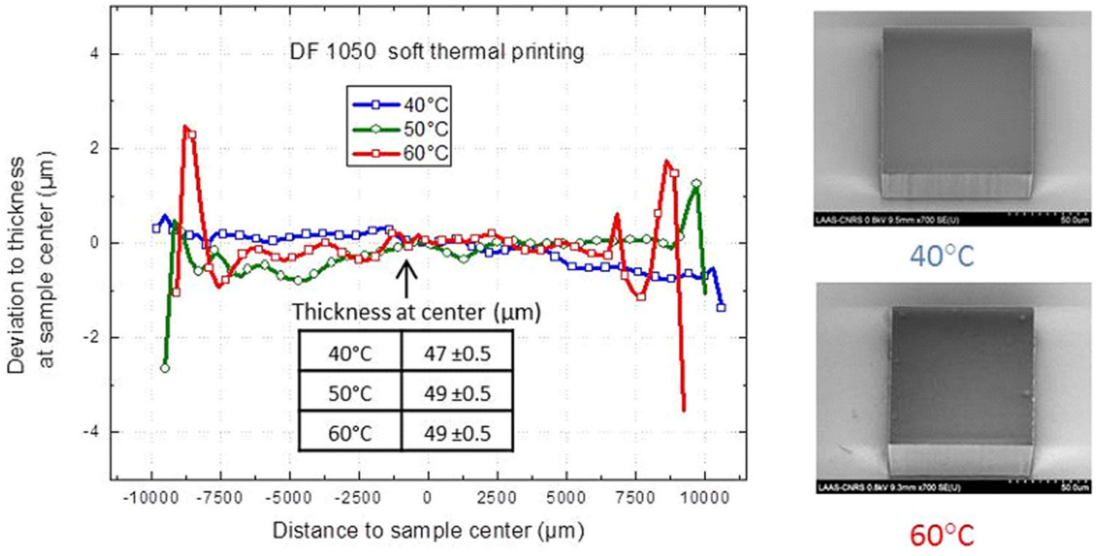

Figure 4: (left) Deviation to the thickness at the centre measured as a function of distance to the sample centre for soft thermal printing of a DF-1050 dry film on a 25x25 mm² silicon sample at 40, 50 and 60°C; (right) Scanning electron microscope (SEM) images of the final posts for lowest and highest STP temperatures (post size: 100x100 µm²). Table inset: thickness measured at the sample centre.

3.2. Optimization of the lamination conditions

Standard lamination was performed on similar samples to serve as a reference. We used a Shipley 360/N laminator and followed the protocol described in figure 2. The photolithography conditions were identical to those used for the STP study (see section 2). Taking into account the recommendations of the dry film manufacturer, the pressure and speed of the rollers were set to 2.5 bars and 0.5 m/min, respectively. Lamination temperature was varied in the available range of the laminator and three temperatures were tested: 65°C, 100°C and 130°C. This range was not exactly equivalent to the one investigated for STP. The difference is due to the fact that in the case of lamination, the temperature was measured on the roller and was much higher than the effective temperature (i.e., at the interface between the substrate and dry film), whereas the temperature for STP was measured closer to the sample using an *in situ* thermocouple. As performed for STP, samples were characterized by mechanical profilometry (figure 3f). The thickness measured at the sample centre was found to fit the expected range (see the table in figure 5).

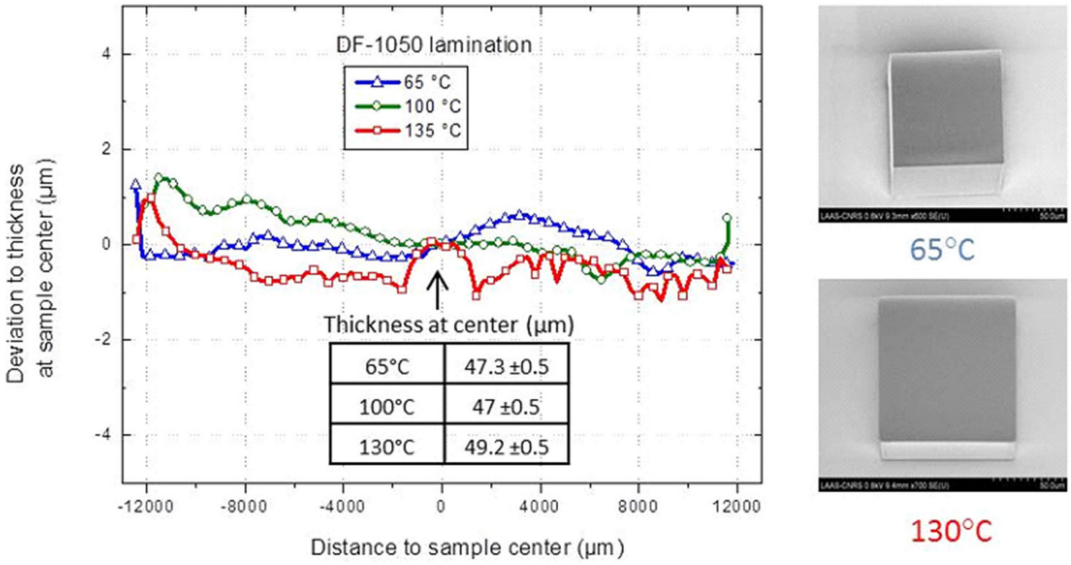

Figure 5: (left) Deviation of the thickness at the centre measured as a function of distance to the sample centre for the lamination of a DF-1050 dry film on 25x25 mm² silicon samples at 65, 100 and 130°C; (right) Scanning electron microscope (SEM) images of the final posts for the lowest and highest lamination temperatures (post size: 100x100 µm²). Table inset: thickness measured at the sample centre.

Figure 5 also shows the evolution of the pattern thickness measured as a function of the distance to the centre for each tested condition. Lamination was not as sensitive to temperature variation as STP, with a maximum deviation to the centre of 1.3 µm, regardless of the applied conditions. Finally, for STP, the SEM images showed satisfactory pattern definition. Nevertheless, because in some cases poorer adhesion was observed for the lowest tested temperature, the lamination temperature was set to 130°C for the rest of the study to ensure optimal adhesion on the sample surface.

3.3. Comparison of the thickness profiles produced by both methods and by standard SU-8 spin-coating

Figure 6 compares the thickness uniformity profiles obtained for both transfer methods in the best conditions tested (i.e., 40°C for STP and 130°C for lamination). A typical profile obtained with a 50-µm-thick SU-8 layer spin-coated on a similar surface is also plotted for comparison. For all methods, the thickness measured at the centre is close to the target value. However, its variation along the sample surface is very different depending on whether a transfer method or spin-coating is used. A maximum thickness variation of 2.6% was found for lamination and 2.9% for STP, compared to greater than 40% in the case of SU-8 spin-coating. Therefore, both lamination and STP significantly improve the thickness uniformity in the case of small-sized samples.

It is worth noting that other types of thick epoxy dry films than the DF-1050 series, such as SUEX films (DJ DevCorp), can also be used with these methods[24][25]. These films are often provided as precut sheets to a size equal to or slightly smaller than the sample, whereas DF-1000 series films are provided in a roll form and generally have to be cut along the sample edges after lamination. One of the main interests in using precut sheets is to avoid material waste. However, positioning a precut sheet during lamination is challenging, especially for small samples. Therefore, to make a precise comparison of both transfer methods possible, we only used DF-1050 films in this study.

Finally, we verified that the optical losses of cured DF-1050 films at 850 nm are similar to those of cured SU-8 (<3 dB cm^{-1}). These films can therefore replace SU-8 for MOEMS integration on VCSELs. In the next section, lamination and STP methods are evaluated for the fabrication of DF-1050 films-based MOEMS arrays on small-sized GaAs samples.

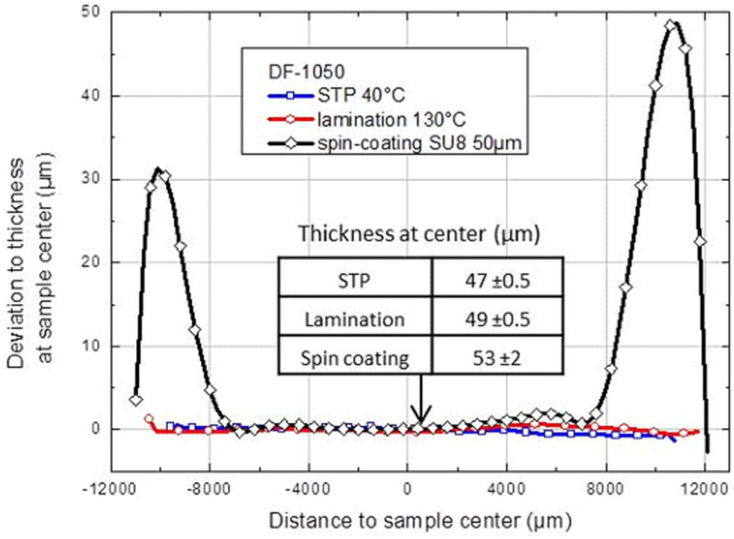

Figure 6: Comparison of lamination and soft thermal printing of a DF-1050 dry film on 25x25 mm² silicon samples under the optimized conditions. A typical profile for standard spin-coating of a 50-µm-thick SU-8 layer on the same surface is also plotted. Table inset: thickness measured at the sample centre.

4. Application to the fabrication of polymer MOEMS on small-sized GaAs samples

4.1. Development of a new MOEMS fabrication process

The MOEMS fabrication process that was previously demonstrated by the authors using spin-coated SU-8 is simple [2]. It requires two successive UV exposures of a single SU-8 layer: a first standard exposure at 365 nm to define the 100-µm-thick anchors (figure 7b) and a second exposure, corresponding to the thin membrane definition, through another photomask at a shorter wavelength (320 nm, due to an optical filter placed in the optical path of the mask aligner), for which the resist has greater absorbance (figure 7c). Membrane release is achieved after resist development. This process was adapted to make it

possible to use dry films (Figures 7 and 8). As DF-1050 films series are not available in a 100-µm thickness range, two successive transfers of two 50-µm-thick films were performed to replace the spin-coated 100-µm-thick SU-8 resist (figure 7a). Note that stacking two films had no impact on the final optical properties of the MOEMS as the junction between the two films remained outside the optical axis after fabrication (figure 8). Identical conditions were used for each successive transfer, i.e., 2x130°C for lamination and 2x44°C for STP case, as these conditions produced the best uniformity results. The photolithography conditions were also adapted for the case of DF-1050 dry films, with exposure doses of 375 mJ/cm² at 365 nm (figure 7b) and of 8 mJ/cm² at 320 nm (figure 7c). Finally, the electrode fabrication step was also optimized (figure 7d). First, a titanium layer was deposited to serve as an actuation electrode material (50 nm). Second, a thicker gold layer (300 nm) was deposited to localize the power dissipation within the suspended areas [26]. These two metallization steps were achieved before DF-1050 development. This new "planar" process enhanced both electrode alignment and definition and completely suppressed the risk of an unwanted metallization below the membrane (i.e., in the optical axis). Two local selective wet etchings were then performed to define the gold pads and the titanium electrode (figure 7e). The development and baking conditions were identical to those in section 2. A final hard bake was added to the end of the MOEMS fabrication (120°C, 2 min) (figure 7f).

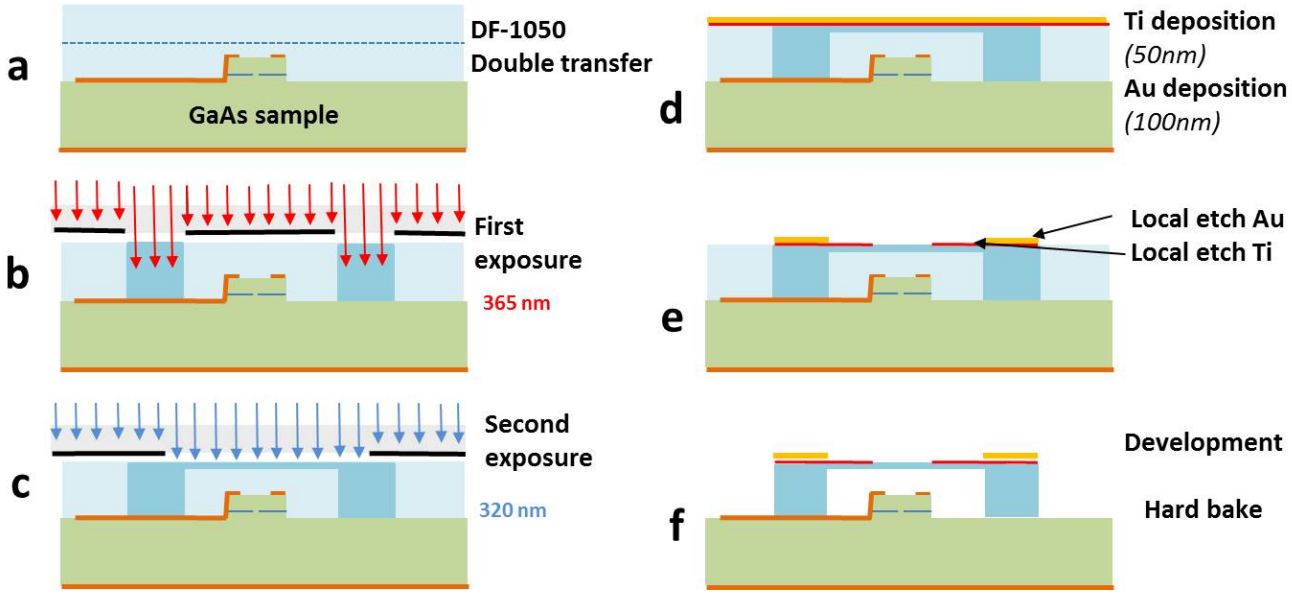

Figure 7: Description of the complete planar process developed for MOEMS fabrication: (a) DF-1050 double lamination or double STP, (b) first UV exposure, (c) second UV exposure, (d) Ti and Au deposition, (e) metal openings through local wet etchings, and (f) development and baking.

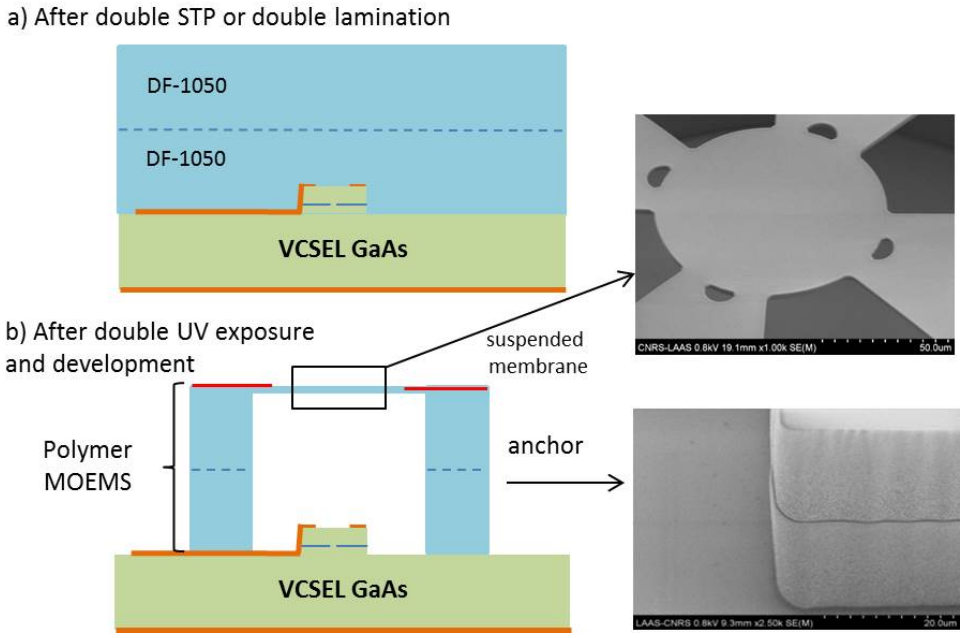

Figure 8: Details of MOEMS fabrication using a double DF-1050 film transfer; (b) SEM observation after stacking two DF-1050 films by STP or by lamination after the anchor and membrane definition by double UV exposure.

4.2. MOEMS characterization

MOEMS arrays were fabricated after double lamination or double STP on several quarters of GaAs wafers of 2 inches in diameter. Pattern definition was observed by SEM after membrane fabrication for each method and was found to be as good as that previously obtained by the authors using SU-8 spin-coating on large 4" silicon wafers (figure 9). Mechanical profilometry was used to determine the MOEMS height on the whole sample surface, which was found to be 95±2.5 µm for each case, in good agreement with the desired values. These results confirm that high aspect ratio devices can be fabricated with high thickness uniformity on small-sized samples by combining lamination or STP with a dry film stacking strategy. Finally, the roughness of the bottom surface of the membrane fabricated by double UV exposure was characterized using atomic force microscopy (AFM) on a reversed MOEMS device peeled from the substrate. An average roughness of 5 nm was measured. This value is similar than that observed for the top surface and is compatible with the micro-optical application aims.

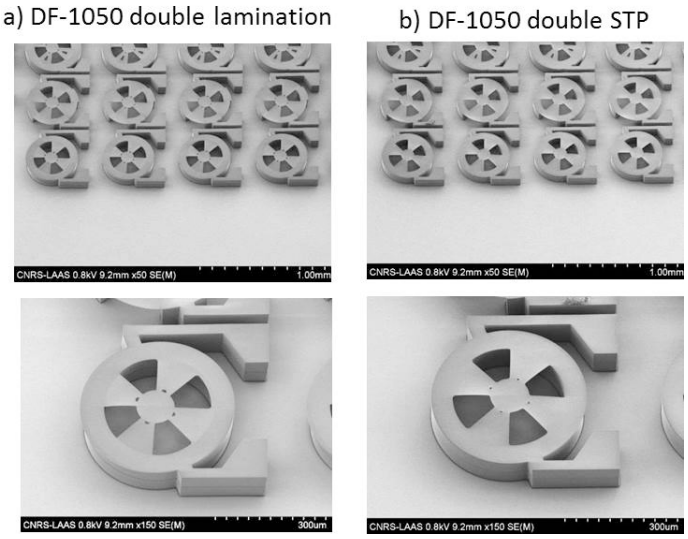

Figure 9: SEM observation of MOEMS arrays fabricated using (a) double lamination and (b) double STP of two stacked DF-1050 films on a GaAs sample (quarter of wafer of 2" in diameter). Anchor height was measured to be 95 µm±2 µm on the whole sample in both cases.

Finally, a typical top view of complete MOEMS arrays, including actuation electrodes fabricated using our planar process, can be seen in figure 10a. The electro-thermal response of such MOEMS was

characterized using an optical profilometer under probes. As seen in figure 10b, a maximal vertical displacement of ~8 µm was obtained for an actuation power of only 12 mW in both cases. These performances are in good agreement with the theoretical behaviour expected for this optimized design [26]. Moreover, the standard deviation of the measured displacement to its average value was equal or less than 0.5 µm, demonstrating the good reproducibility achievable using dry resist films for MOEMS fabrication process.

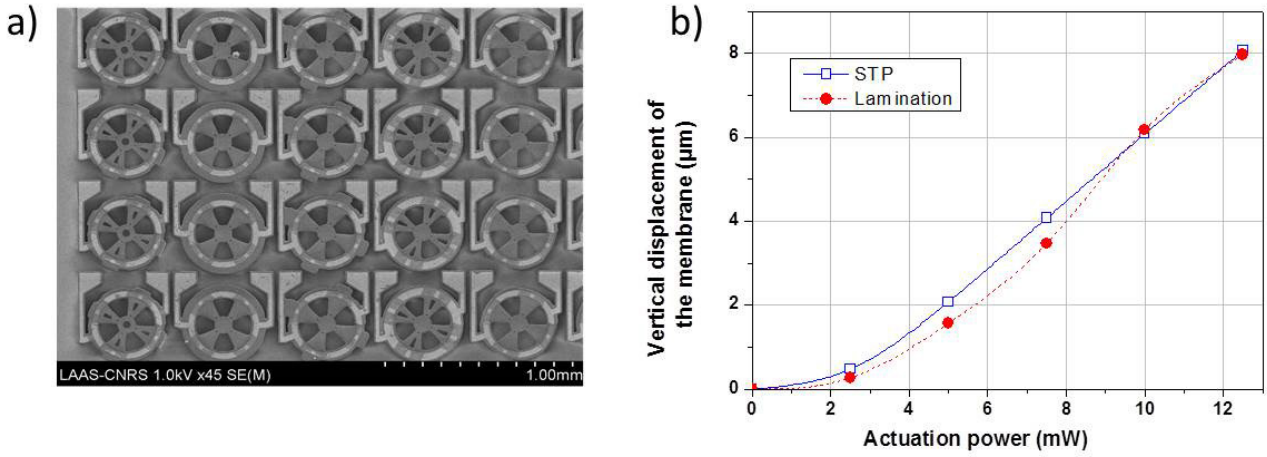

Figure 10: a) SEM view of complete MOEMS arrays fabricated using double STP; b) Typical vertical displacement of the membrane measured under probes as a function of the actuation power for MOEMS fabricated by lamination and by STP.

5. Conclusions

STP was applied to the transfer of commercial thick dry photoresist films (DF-1050 series) on small-sized samples (25x25 mm²) to avoid the edge beads at the sample periphery that are produced via standard spin-coating of SU-8. The uniformity results were compared to those obtained with lamination under similar conditions. For both methods, it was possible to obtain thickness variation as low as 3% along the whole sample, compared to the greater than 40% variation obtained by SU-8 spin-coating on the same surface. Lamination and STP were then applied to the fabrication of high aspect ratio polymer-based MOEMS arrays on small GaAs samples (quarters of wafers of 2 inches in diameter) via the stacking of

two DF-1050 films and double UV exposure. In both cases, the device height was in agreement with the targeted value over the whole sample surface, whereas the thickness inhomogeneity significant in the case of SU-8 spin-coating. Finally, MOEMS arrays were fabricated using a planar fabrication process. Reproducible electro-thermo-mechanical behaviour was observed whether lamination or STP was used. This study demonstrates the potential of dry thick film transfer techniques for micro-optics/MOEMS collective fabrication. Since optoelectronic devices are fabricated on brittle III-V semiconductor substrates (GaAs, InP) and STP is softer and requires less sample manipulation, future work will address the final integration of MOEMS arrays on GaAs-based VCSELs by means of STP of two stacked DF-1050 films.

ACKNOWLEDGEMENTS

The authors gratefully acknowledge RENATECH (French Network of Major Technology Centres) within LAAS-CNRS for technological support. The French National Research Agency (ANR) is also gratefully acknowledged for financial support (ANR-14-ASTR-0007 HYPOCAMP and ANR-15-CE19-0012 DOCT-VCSEL). The authors would also like to thank Samuel Charlot, Laurent Mazenq and Adrian Laborde for their help with the fabrication steps.

REFERENCES

[1] R. Michalzik "VCSELs: A Research Review" in Fundamentals, Technology and Applications of Vertical-Cavity Surface-Emitting Lasers. Springer, pp. 1-17, 2013

[2] B. Reig, V. Bardinal, T. Camps, Y. G. Boucher, C. Levallois, J. B. Doucet, D. Bourrier, E. Daran, J. Launay " Polymer tunable microlens arrays suitable for VCSEL beam control" Proc. SPIE 8428, Micro- Optics 2012, 84280N (June 1, 2012)

[3] B Reig, T Camps, V Bardinal, D Bourrier, E Daran, J B Doucet, J Launay and J Y Fourniols "Fabrication of polymer-based optical microsystem arrays suited for the active focusing of vertical laser diodes"2012 J. Micromech. Microeng. 22 065006.

[4] H. Lorenz, M. Despont, N. Fahrni, N. Labianca, P. Renaud, and P. Vettiger, "A low cost negative resist for MEMS", J. Micromechanical Microengennering 7, 121-124, (1997)

[5] H. Lorenz, M. Despont, N. Fahrni, J. Brugger, P. Vettiger, P. Renaud, "High aspect-ratio, ultrathick, negative-tone near-UV photoresist and its applications for MEMS", Sensors and Actuators A 64, 33-39, (1998)

[6] E. H. Conradie and D. F. Moore "SU-8 thick photoresist processing as a functional material for MEMS applications" Journal of Micromechanics and Microengineering Volume 12 Number 4 2002, J. Micromech. Microeng. 12 368

[7] J. Hsieh, C.-J. Weng, H.-L. Yin, H.-H. Lin, H.-Y. Chou, "Realization and characterization of SU-8 micro cylindrical lenses for in-plane micro optical systems", Microsystem Technologies 11, 429–437, (2005)

[8] A. Nallani, T. Chen, J.-B. Lee, D. Hayes and D. Wallace, "Wafer level optoelectronic device packaging using MEMS", Proc. SPIE 5836, 116 (2005)

[9] A.Gracias, N. Tokranova, and J. Castracane "SU8-based static diffractive optical elements: wafer-level integration with VCSEL arrays" Proc. SPIE 6899, 68990J (2008)

[10] V. Bardinal, B. Reig, T. Camps, C. Levallois, E. Daran, C. Vergnenègre, T. Leïchlé, G. Almuneau, and J.-B. Doucet. "Spotted Custom Lenses to Tailor the Divergence of Vertical-Cavity Surface-Emitting Lasers" IEEE Photon. Technol. Lett., 22, 21, 1592-1594, (2010)

[11] Y.-J. Chuang, F.-G. Tseng, W.-K. Lin Microsystem ”Reduction of diffraction effect of UV exposure on SU-8 negative thick photoresist by air gap elimination” Microsystem Technologies 8 (2002) 308-313

[12] Zhang, J.; Chan-Park, M.B.; Jianmin Miao; Sun, T.T., "Reduction of diffraction effect for fabrication of very high aspect ratio microchannels in SU-8 over large area by soft cushion technology", Microsystem Technologies, 11 (7): 519-525 (2005)

[13] R. Yang, C. Mullen, M. Schaline, K. Reithmaier and R. Sheets, "High throughput projection UV lithography of high-aspect-ratio thick SU-8 microstructures", Microsystem Technologies 14 (2008) 1233–1243

[14] C. Levallois, V.Bardinal, C.Vergnenegre, TLeïchlé, T.Camps, E.Daran, J-B.Doucet “VCSEL collimation using self-aligned integrated polymer microlenses” SPIE 6992 69920W (2010)

[15] H. Lee, K. Lee, B. Ahn, J. Xu, L. Xu and K. WOh “A new fabrication process for uniform SU-8 thick photoresist structures by simultaneously removing edge bead and air bubbles “ J. Micromech. Microeng. 21 (2011) 125006

[16] J.Kim, P.Jao, C.Kim , Y.Yoon “Dispense and self-planarization process on a modified surface for multiple height 3-D microfabrication “ 16th International Solid-State Sensors, Actuators and Microsystems Conf. (Beijing), pp.1372,1375 (2011)]

[17] D. Bourrier et al “Potential of BPN as a new negative photoresist for a very thick layer with high aspect ratio”, Microsyst. Technologies, 2014, Volume 20, Issue 10, pp 2089-2096

[18] N. P. Pham, J. N Burghartz and P. M. Sarro “Spray coating of photoresist for pattern transfer on high topography surfaces “J. Micromech. Microeng.Volume 15 Number 4 15 691 (2005).

[19] P. Vulto, N. Glade, L. Altomare, J. Bablet, G. Medoro, A. Leonardi, A. Romani, I. Chartier, N. Manaresi, M. Tartagni and R. Guerrieri “Dry film resist for fast fluidic prototyping”. Proc. MicroTAS 2004, Malmö : Sweden, p 43-45 (December 2004)

[20] P. Abgrall, C. Lattes, V. Conédéra, X. Dollat, S. Colin and A.M. Gué, “A novel fabrication method of flexible and monolithic 3D microfluidic structures using lamination of SU-8 films” J. Micromech. Microeng. 16 113–21 (2006).

[21] S. Abada, B. Reig, E. Daran, J.B. Doucet, T. Camps, S. Charlot, V. Bardinal, "Uniform fabrication of thick SU-8 patterns on small-sized wafers for micro-optics applications" SPIE Photonics Europe (pp. 91300R-91300R). International Society for Optics and Photonics (2014, May)

[22] EMS Adhesives (Delaware, OH, USA) (http://emsadhesives.com)

[23] R.Courson , S.Cargou, V.Conédéra , M.Fouet , C. Blatché, C.L.Serpentini, A-M. Gué ,"Low-cost multilevel microchannel lab on chip: DF-1000 series dry film photoresist as a promising enabler" Advances, Royal Society of Chemistry , 4 (97), pp.54847-54853 (2014)

[24] D.Johnson, A.Voigt, G.Ahrens, W.Dai, "Thick Epoxy Resist Sheets for MEMS Manufacturing and Packaging", 2010 IEEE 23rd International Conference on Micro Electro Mechanical Systems (MEMS) (Wanchai, Hong Kong), p.412,415

[25] S. Abada, L. Salvi, E. Daran, R. Courson, B. Reig, J.B. Doucet, T. Camps, S. Charlot, V. Bardinal, "Comparison of soft thermal printing and lamination for the fabrication of high aspect ratio patterns on small-sized samples" International Conference on Micro and Nano Engineering (MNE) 2015 La Haye, N° 15337 (September 2015)

[26] Tan H, Kong L, Li M, Steere C, Koecher L 2004 Current status of Nanonex nanoimprint solutions Proc. SPIE 5374

[27] S.Abada, T.Camps, B.Reig, J.B.Doucet,E.Daran, V.Bardinal "3D optimization of a polymer MOEMS for active focusing of VCSEL beam", SPIE Proc. SPIE 9130, Micro-Optics 2014, 913003 (2 May 2014)